Jinst

Published by IOP Publishing for Sissa Medialab

Received: *February 6, 2023*
Accepted: *April 2, 2023*
Published: *April 26, 2023*

High-efficiency recovery of ^{82}Se from enriched Zn^{82}Se scintillating bolometer crystals

S.S. Balabanov,[a] **B. Broerman,**[b] **I. Dafinei,**[c] **S.V. Filofeev,**[a] **M. Laubenstein,**[d] **S.S. Nagorny,**[b,e,*] **S. Nisi,**[d] **L. Pagnanini**[c] **and S. Pirro**[d]

[a] *G.G. Devyatykh Institute of Chemistry of High-Purity Substances of the Russian Academy of Sciences, 49 Tropinin Str., 603950 Nizhny Novgorod, Russia*
[b] *Department of Physics, Engineering Physics and Astronomy, Queen's University, 64 Bader Lane, K7L 3N6 Kingston, ON, Canada*
[c] *Gran Sasso Science Institute, viale Francesco Crispi 7, 67100 L'Aquila, AQ, Italy*
[d] *INFN — Laboratori Nazionali del Gran Sasso, via Giovanni Acitelli 22, 67100 Assergi, AQ, Italy*
[e] *Arthur B. McDonald Canadian Astroparticle Physics Research Institute, 64 Bader Lane, K7L 3N6 Kingston, ON, Canada*

E-mail: sn65@queensu.ca

Abstract: As experiments searching for neutrinoless double beta decay push into the inverted hierarchy, enriched isotope target masses of hundreds of kilograms are required. Due to unavoidable losses throughout the entire production chain, the recovery of expensive enriched material used in crystal-based experiments should be given special attention. The CUPID-0 experiment using Zn^{82}Se scintillating bolomoters provides a unique opportunity at the 10-kg-scale to test a recovery process for enriched ^{82}Se. We present a multi-stage, high-yield method consisting of wet chemistry and vacuum distillation. The chemical purity, isotopic abundance, and radiopurity is demonstrated to be preserved after the ^{82}Se extraction with recovery efficiency no less than 86.4% (that potentially can be higher than 94.7%) and chemical purity of 99.999%.

Keywords: Double-beta decay detectors; Materials for solid-state detectors; Gamma detectors (scintillators, CZT, HPGe, HgI etc)

*Corresponding author.

https://doi.org/10.1088/1748-0221/18/04/P04035

2023 JINST 18 P04035

Contents

2023 JINST 18 P04035

1 Introduction

The neutrino is a key particle in astroparticle physics and cosmology, but despite extensive studies some of its fundamental properties are still not well understood. Strong evidence that neutrinos have non-degenerate mass comes from the observation of neutrino flavor oscillations in experiments looking at solar, atmospheric, and reactor neutrinos [1]. Neutrino oscillations have motivated a worldwide experimental effort to measure its absolute mass and the actual scheme of the neutrino mass hierarchy. Neutrinoless double beta decay (0ν-DBD) is the only practical path to determine the nature of the neutrino (Dirac or Majorana) and one of the most sensitive probes of its absolute mass [2]. If 0ν-DBD is observed, this would imply the Majorana nature of the neutrino and lepton number violation, which could lead to an explanation for the matter-antimatter asymmetry in the Universe [3]. Therefore the search for 0ν-DBD with different target isotopes is a top priority according to recommendations of APPEC committee [4].

Currently-running and planned 0ν-DBD experiments aim to reach an experimental sensitivity in terms of half-life at the order of $10^{27} - 10^{28}$ yr to probe the inverted neutrino hierarchy [2]. Such experimental sensitivity could be achieved only in a well-shielded experimental setup located deep underground and operating a ton-scale detector with excellent performance, produced from a highly chemically-, radio-pure, and enriched DBD-active isotope. To reach such ultimate sensitivity, special care has to be taken at each step of the detector development, from its production to operation, in order to minimize any possible losses of enriched material and to reduce its radioactive contamination.

Large-scale 0ν-DBD experiments using a noble gas targets in a loaded scintillator (KamLand-Zen [5], THEIA [6]), a single/dual-phase cryogenic liquid or high-pressure gas time projection chambers (EXO-200 [7], NEXT-White [8], PandaX-II [9], nEXO [10], NEXT-1T [11], XENON1T [12])

will not face the same issues in the recovery of enriched isotopes as any crystal-based experiments. The processing systems used in these experiments are highly efficient in delivering gas from the purification system to the detector and back to storage or recovery systems preserving the chemical purity of enriched isotopes. In case of crystal-based experiments, such as LEGEND [13] (high purity ^{76}Ge), AMoRE [14] ($Li_2{}^{100}MoO_4$, $Ca^{100}MoO_4$), CUPID-Mo [15] and CUPID [16] ($Li_2{}^{100}MoO_4$) the situation is more complex and requires dedicated experimental programs for the development of an efficient recovery procedure for the $O(100)$ kg of enriched isotopes to be deployed. Crystalline materials require multi-step procedures including original compound decomposition, enriched isotope separation followed by its thorough purification, and a dedicated storage approach. Moreover, the production yield of high quality crystals that would fully satisfy the strict requirements of low-background experiments and could be used "as-produced" typically do not exceed (40 – 50)% of the initially used isotope mass. Therefore, the appropriate use of the whole amount of an expensive enriched isotope would lead to an increase of nuclei of interest, translating to a higher experimental sensitivity. It is therefore advantageous to develop a technology to extract an enriched isotope from any remnants of crystal growth and crystal conditioning processes, and to re-use it again.

The CUPID-0 experiment [17], taking data within 2017 – 2020, was the first kg-scale demonstrator taking advantage of ZnSe crystals produced from selenium highly enriched in the ^{82}Se isotope accompanied by the benefits of operating these crystals as scintillating bolometers with an extremely effective particle identification capability. Challenges during the production of 24 enriched and 2 natural ZnSe crystals with total mass of 10.5 kg corresponding to 5.17 kg of ^{82}Se using 15 kg of initial ^{82}Se isotope are described in detail in [18]. The solutions found for problems encountered in constructing the CUPID-0 detector are of particular interest because similar issues will arise in future ton-scale experiments, regardless which enriched isotope is being studied.

Here we focus on the recovery of the ^{82}Se isotope and present a method of high-yield recovery from the approximately 12 kg of various remnants obtained during the enriched $Zn^{82}Se$ crystal production in the framework of the CUPID-0 experiment. This paper is organized as follows: in section 2 we discuss the growth procedure of $Zn^{82}Se$ crystals; the extraction technique for the ^{82}Se is presented in section 3; chemical purity, isotopic composition, and radiopurity at each stage is evaluated and is presented in section 4; and a discussion and conclusions is presented in section 5.

2 ZnSe crystal growth

The $Zn^{82}Se$ crystals were the core of the CUPID-0 experiment acting as cryogenic scintillating bolometers. This detector technique is commonly used in rare event searches [19, 20]. Since ZnSe crystals are both the source of the decay and the detector material, several requirements should be fulfilled to achieve the ultimate experimental sensitivity. First, to enhance the detection efficiency of the two electrons emitted in the 0ν-DBD, up to (80 – 90)%, crystals of a relatively large dimensions (diam. 40 – 45 mm and 55 – 60 mm in length, with mass more than 450 g) are required. Secondly, the presence of bulk defects like bubbles, inclusions, veils or cracks, as well as intrinsic point defects should be minimized as they may drastically affect the phonon propagation in the crystal [21]. As a result, the thermal conductivity of the detector material decreases while the heat capacity increases, causing a loss in the signal amplitude and energy resolution in the heat channel of such phonon-mediated detectors [22]. Another important aspect related to scintillation light propagation

2023 JINST 18 P04035

and collection is a good optical transmittance (the bulk absorption coefficient should be less than 0.5 cm^{-1} at 630 nm) to avoid re-absorption of the scintillation light that would decrease the particle identification provided by the light signal characteristics (for more details on studies of ZnSe optical and luminescence properties see [18, 23]).

The $Zn^{82}Se$ scintillating crystals used in the CUPID-0 experiment were grown from a melt in graphite crucibles using the High-Pressure Bridgman-Stockbarger technique [24, 25]. The growth process was performed in vertical two-zone furnaces kept under high pressure of argon (up to 1.5 MPa) with a typical growth rate of 1 mm/hour. The growth of large-volume ZnSe crystals from the melt is difficult due to its high melting point (1525°C) and high total vapor pressure (0.2 MPa at 1525°C) [25]. It is further complicated by the high volatility of the initial charge components, i.e. Zn and ^{82}Se, which have different vapor pressures leading to a deviation from the stoichiometric composition of the melt during the growth process.

Despite ZnSe crystals having many applications in IR optics, optoelectronic devices, X-ray and soft gamma-ray detection, they are quite seldom produced in the form of a large volume single crystals. Typical dimensions are not exceeding 40 mm in diameter and 50 mm in length. Therefore, $Zn^{82}Se$ crystals production in the framework of the CUPID-0 experiment apart from various technological issues connected with the growth of large-volume high-quality and high-purity crystals, also met difficulties arising from the need to minimize losses of the enriched ^{82}Se isotope at all production stages.

The method of initial material preparation, conditioning, and $Zn^{82}Se$ crystal growth is well-described in [18]. In view of the enriched selenium recovery we need to keep in mind the yield in three main stages of the crystal production: charge synthesis from initial materials, crystal growth, and crystal processing and conditioning. The total yield of the $Zn^{82}Se$ powder synthesis and conditioning for the crystal growth was 98.35%.

The total yield of the "as-grown" $Zn^{82}Se$ crystalline ingot production was estimated over 28 growth processes as 78% from the initially-loaded charge. As previously mentioned, the high volatility of both initial elements (^{82}Se and Zn) at the compound melting point, leads to complexity in the $Zn^{82}Se$ crystal growth, as well as results in an evaporation of approximately 17% of the initially loaded $Zn^{82}Se$ charge. This sublimate, of a very complex composition, that could slightly vary from one growth to another, precipitates inside the graphite crucible (~12%) and outside of the graphite crucible (~5%) penetrating through its porous walls onto all "cold" parts of the furnaces' inner volume, which have a temperature below its condensation point. After being collected, this latter fraction of the remnants was full of carbon from the heating element material (graphite) and the thermal insulation (carbon felt). The remaining 5% of the initially-loaded $Zn^{82}Se$ charge was lost due to its condensation on elements and materials of the inner volume of the furnaces where it cannot be collected.

All ^{82}Se-containing materials carefully collected at each processing stage of the $Zn^{82}Se$ crystal production were grouped in several categories of waste according to their expected chemical and isotopic purity. Each category was subjected to a separate recovery process, starting from the most clean fraction to the most dirty one. We refer to the three categories as primary, secondary, and tertiary batches.

The primary batch consists of: a) crystals as a result of an unsuccessful growth, i.e. crystalline boules which were so defective that have been immediately subjected to the recycling processes; b)

2023 JINST 18 P04035

crystal pieces which were cut from "as-grown" ingots during shaping of the $Zn^{82}Se$ crystal (nose, tail, some parts of the boules cut due to defects like bubbles, voids, inclusions, or cracks); c) $Zn^{82}Se$ sublimate, collected from the inner volume of graphite crucibles; d) remnants of high quality $Zn^{82}Se$ charge powder.

The secondary batch consists of: a) $Zn^{82}Se$ sublimate collected outside of the crucible in the inner volume of the furnaces; b) residuals from $Zn^{82}Se$ charge powder production; c) all possibly ^{82}Se-containing materials from synthesis, conditioning, growth stage, etc.

The tertiary batch consists of remnants obtained during the crystal cutting and polishing, which is a water suspension with a small fraction of $Zn^{82}Se$ particulates. During all mechanical treatment of $Zn^{82}Se$ crystals, water was used as lubricant and coolant. All water used in cutting or polishing procedures was collected in a 1 m^3 plastic water tank allowing for the extraction of ^{82}Se from this water waste.

All steps in the processing chain of $Zn^{82}Se$ crystal production leads to a significant amount of remnants and waste. Each type of waste had a specific chemical form, impurity concentration, and selenium isotopic composition. Therefore, a recovery technique should provide a high flexibility to be applied to each type of remnants with the same ultimate efficiency.

3 Extraction technique

The extraction technique developed here combines several methods. A sequence of wet chemistry reactions in order to effectively extract elementary selenium is followed by a multi-stage vacuum distillation to achieve the ultimate chemical and radio-purity level of the material.

3.1 Wet chemistry

The aim of the first stage of wet chemistry reactions was to convert the selenium into a soluble form. Batches of 300 g of Se-containing material were placed in a flask with a reflux condenser (made of heat-resistant borosilicate glass) and then concentrated nitric acid (6N purity grade, SigmaTec, Russia) was added drop-wise until nitrogen dioxide emanation was stopped following the redox reaction:

$$ZnSe + 8HNO_3 \rightarrow H_2SeO_3 + Zn(NO_3)_2 + 6NO_2\uparrow + 3H_2O. \tag{3.1}$$

The resulting solution was separated from the insoluble impurities on a Nutsche filter (made of heat-resistant borosilicate glass) and the precipitate rinsed several times with deionized water (with specific resistivity of 18.2 MΩ cm) for a more complete removal of the selenous acid. Then, water from this solution was evaporated in a quartz beaker at approximately 90°C, and afterwards the zinc nitrate salt and selenous acid were decomposed at approximately 300°C, for several hours according to reactions (3.2):

$$\begin{cases} 2Zn(NO_3)_2 \rightarrow 2ZnO\downarrow + 4NO_2\uparrow + O_2\uparrow, \\ H_2SeO_3 \rightarrow SeO_2\downarrow + H_2O\uparrow . \end{cases} \tag{3.2}$$

2023 JINST 18 P04035

The resulting ZnO and SeO_2 precipitates were then dissolved in a concentrated hydrochloric acid (5N purity grade, SigmaTec, Russia):

$$\begin{cases} ZnO + 2HCl \rightarrow ZnCl_2 + H_2O, \\ SeO_2 + H_2O \rightarrow H_2SeO_3. \end{cases} \tag{3.3}$$

At the last stage the selenium was reduced by a hydrazine hydrate (4N purity grade, LenReaktiv, Russia), added drop-wise to the solution, according to the reaction [26, 27]:

$$H_2SeO_3 + N_2H_4 \rightarrow Se\downarrow + 3H_2O + N_2\uparrow . \tag{3.4}$$

As a result, red amorphous Se precipitates and then solidifies under a slight heating and turns black in colour. The black selenium was separated from the $ZnCl_2$ water solution through another Nutsche filter and washed thoroughly with deionized water. The overall yield of the Se-extraction through the wet chemistry stage of the 300-g-batch was conservatively estimated to be 97% based on the stoichiometric ratio between Zn and Se.

3.2 Vacuum distillation

To prepare the selenium for further purification it was distilled under a high purity argon flow (1 L/hour) in a quartz ampule of a dedicated design. The Se was heated to near its boiling point (660°C) and excess humidity was driven off with an argon flow. The Se vapour then condensed as droplets in the capillary nose of the ampule before dropping into a beaker of deionized water acting as a coolant. This step produces Se granules of approximately 3-mm-diameter.

The resulting Se granules were then ready for treatment with a multi-stage vacuum distillation developed based on earlier studies [28, 29]. A schematic view of the distillation apparatus, made of quartz, is shown in figure 1. The granules were first loaded into the vessel 1 through side A. In the first step the entire system was heated at (150 – 180)°C and evacuated to a residual pressure of 3×10^{-6} mm Hg. The temperature was then raised to 250°C to melt the Se and then held for 6 hours at this temperature under high vacuum to degas the Se melt. Next, the temperature in feed vessel 1 was increased to 370°C to transfer the Se vapour to vessel 2 that was kept at 260°C to condense Se. The specific evaporation rate achieved during this step was 1.3×10^{-3} cm^3/cm^2s. After the end of this transfer stage vessel 1 was soldered off.

Next was a purification step to remove hydrogen-, sulfur-, and carbon-containing impurities performed in vessel 2 and condenser 3. Helium gas containing 5 vol.% oxygen was fed from side B at 0.8 bar. Vessel 2 was maintained at 660°C for 18 hours and condensation performed at 300°C on the condenser 3. At this stage, the temperature in vessels 4 – 7 was kept at 350°C. The presence of oxygen forces hydrogen, sulfur, and carbon to form compounds with various oxidation states. After processing the temperature of selenium melt in vessel 2 was decreased to 350°C, and the system was evacuated through side B freezing volatile reaction products and possible admixture of selenium dioxide in the liquid-nitrogen filled trap 8.

After the oxidation of impurities and their removal, Se in vessel 2 was kept under vacuum pumped from side B. High vacuum distillation of the selenium was then carried out from vessel 2 to vessel 4, vessel 4 to 5, and 5 to vessels 6 and 7 by maintaining the necessary temperature gradient of selenium melt from 370°C to 350°C resulting in a sequentially-decreasing evaporation rate of

2023 JINST 18 P04035

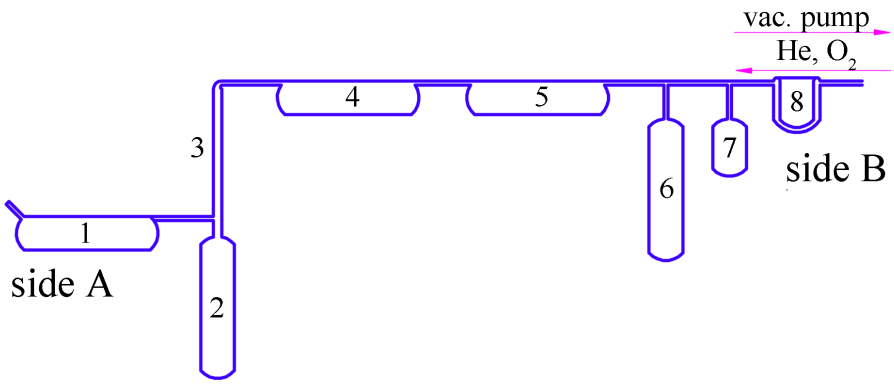

Figure 1. Flow diagram of the distillation apparatus with a feed vessel for initial loading of the selenium (1), vessel (2) and condenser (3) for gas treatment of the selenium melt, vessels (4 and 5) for sequential high-vacuum distillation, a receiver for the purified selenium (6), a collection vessel witness samples (7), and a trap (8) cooled with a liquid nitrogen.

1.5×10^{-4} cm^3/cm^{2}s, 8.5×10^{-5} cm^3/cm^{2}s, and 1.7×10^{-5} cm^3/cm^{2}s, respectively. After the transfer from each vessel, the previous vessel was soldered off to separate non-volatile contaminants from the distillation apparatus. The purified ^{82}Se was recovered in vessel 6 while the Se in vessel 7 was used as a witness sample for ICP-MS analysis. The total duration of the multi-stage distillation process was approximately 80 hours.

The recovered ^{82}Se ingots were sealed under vacuum to prevent oxidation in large quartz ampules (4 pcs.) with a total mass of 6.51 kg. The ampules were then shipped by land transportation to Laboratori Nazionali del Gran Sasso (LNGS, Italy) and stored underground prior any characterization. The overall yield of the ^{82}Se isotope recovery was estimated only for the primary batch. The total mass of the primary batch before the extraction process was 10130.0 g, which corresponds to 5635.4 g of ^{82}Se assuming the stoichiometric ratio between Zn and Se. The mass of selenium after all processing stages of the recovery process was 4870.0 g. Hence, the effective yield of the enriched selenium recovery for the primary batch was no less than 86.4% and potentially higher. The main uncertainty of the recovery yield value deriving from the accident that happened during the reduction of selenium by a hydrazine hydrate (reaction (3.4)), the exothermic reaction in which the solution temperature can unevenly and abruptly rise. The beaker breaks and the ^{82}Se-containing solution spilled out. These spills were collected, processed separately and then added to the secondary batch, considering preserving the radiopurity of the primary batch of ^{82}Se as a major constraint compared to its reduced mass. After this accident, the reduction process was modified to better control the reaction rate. Taking into account the mass of selenium transferred to the secondary batch, the recovery yield could be estimated as 94.7%. More precise evaluation of the ^{82}Se recovery yield could be done in further studies, taking into account all complications that occurred in the present study. The preliminary ICP-MS measurements to determine the actual stoichiometric ratio and overall chemical purity of each Zn^{82}Se crystal or ^{82}Se-containing remnant with a high precision are also required prior the recovery process.

The yield cannot be evalutated for the secondary and tertiary batches based on the nature of the collection process. However, the mass of ^{82}Se recovered from the secondary batch was measured

2023 JINST 18 P04035

to be 1653.5 g and from the tertiary batch was 133.7 g. Additionally this does not include the approximately 20 g of witness samples used for High Resolution Inductively Coupled Plasma Mass Spectrometry analysis (HR-ICP-MS).

4 Results

The chemical purity, isotopic composition, and radiopurity were evaluated at each step from the initial Zn and Se constituents, to ZnSe crystallization, to ^{82}Se recovery.

4.1 Chemical purity

The concentration of chemical impurities after the purification process in the Se samples of different origin was determined by HR-ICP-MS (Thermo Fisher Scientific ELEMENT2) at the LNGS and are listed in table 1. The analysis was performed in a semi-quantitative mode, calibrating the instrument with a single standard solution containing 10 ppb of Li, Y, Ce and Tl. The uncertainty is approximately 25% of the given concentration values expressed in ppb (i.e. 10^{-9} g of a certain contaminant per 1 g of a studied sample, either ^{82}Se or Zn^{82}Se). It should be noted, that only elements of particular interest were tested at each specific processing stage. Approximately 50 mg of each selenium sample was placed into a plastic vial, filled with 1 ml of nitric acid and placed in an ultrasonic bath at room temperature until full sample decomposition. Vials with samples dissolved in this manner were prepared for a HR-ICP-MS analysis by adding ultra-pure water up to 10 ml of a total volume, with an average dilution factor of approximately 1000.

The chemical purity of the recovered Se from the primary batch is compatible with the purity of the enriched material used for the growth of Zn^{82}Se crystals [18]. The highest concentration of impurities is observed for Te, Zn, Ca and Si at the level of 1.2 ppm, 0.7 ppm, 7.0 ppm and 2.8 ppm, respectively. While Al that was used as dopant in Zn^{82}Se crystals is present at 0.9 ppm.

The secondary batch of Se has a slightly worse final chemical purity. It should be stressed that our Zn^{82}Se crystals were grown in furnaces which are routinely and actively used for the production of ZnSe crystals from natural (non-enriched) selenium and with various dopants (Te, O, Na, Al, Cd, Sm, Fe, Mn) at levels up to a few at.%. Therefore, relatively high concentrations of Na, Al, Te, and other elements (see table 1) in the recovered Se secondary batch is due to the nature of the waste collected from the recycling of the furnace.

The chemical purity of selenium from the tertiary batch varies significantly from the other two batches discussed above. This can be explained, first, from the processing of other crystals ($CdWO_4$, TeO_2, $PbWO_4$) than Zn^{82}Se in the facility over the time of the waste water collection. A high level of Cd, Pb and Te impurities simply reflects their higher initial concentrations in the waste processing water. Secondly, after the wet chemistry stage, as performed for primary and secondary batches, the subsequent vacuum distillation was carried out in a different manner. Due to a low mass of this selenium (just about 150 g), it was purified six times by vacuum distillation at approximately 360°C and under pressure $(2 - 10) \times 10^{-6}$ mm Hg without gas-thermal treatment of the boiled selenium melt.

2023 JINST 18 P04035

Table 1. The concentration (in ppb) of some critical elements presented in the extracted selenium (primary, secondary, and tertiary) batches and measured by a HR-ICP-MS. The concentration of elements was measured in a semi-quantitative mode with uncertainties of approximately 25% ("n.a." stands for "not analyzed"). Data on impurity concentration of the initial ^{82}Se are retrieved from [18].

	Concentration [ppb]				
Element	Initial ^{82}Se	Zn^{82}Se	Primary	Secondary	Tertiary
Na	< 1000	< 300	< 300	1500	n.a.
Mg	< 100	800	400	1500	< 400
Al	< 200	5800	900	1800	< 700
Si	18000	3100	2800	5500	n.a.
S	130000	110000	< 1000	1000	< 40000
K	< 2000	< 1000	< 1000	1000	< 500
Ca	5000	< 4000	7000	7000	n.a.
V	< 40	1	< 1	< 1	< 50
Cr	< 100	< 20	< 20	< 20	< 20
Mn	< 10	6	2	3	< 10
Fe	110	300	100	500	< 200
Co	< 4	1	< 1	1	24
Ni	64	150	200	600	< 200
Cu	< 10	< 200	< 80	< 80	< 20
Zn	n.a.	n.a.	700	2000	250000
As	n.a.	65	80	200	n.a.
Mo	< 10	< 2	6	30	n.a.
Cd	< 4	200	< 5	< 5	600
Te	n.a.	900	1200	57000	90000
Ba	n.a.	250	50	500	< 100
Tl	n.a.	< 0.5	< 0.5	< 0.5	2.5
Pb	< 6	10	15	80	17000
Bi	6	0.5	6	6	n.a.
Th	< 0.1	< 0.2	< 0.2	< 0.2	< 30
U	< 0.1	< 0.2	< 0.2	< 0.2	< 1

4.2 Isotopic composition

The isotopic composition of the recovered selenium samples was studied in complimentary measurements of three different samples from the primary, secondary, and tertiary batches. The ^{82}Se enrichment level was measured by the HR-ICP-MS at LNGS. The results of HR-ICP-MS measurements are presented in table 2.

Evident in table 2 is the conservation of the isotopic abundance of selenium in the primary batch, recovered mostly from pieces of Zn^{82}Se crystals. The initial isotopic abundance is conserved as well in the tertiary batch recovered from the processing water used in all operations for Zn^{82}Se crystals cutting, conditioning and polishing. During the whole cycle of the enriched crystal production no other ZnSe crystals produced from natural selenium or another enrichment level were processed

2023 JINST 18 P04035

Table 2. Isotopic abundance of selenium isotopes in natural and initial ^{82}Se samples [30], enriched Zn^{82}Se [18], and as measured by HR-ICP-MS in the recovered ^{82}Se samples from the primary, secondary, and tertiary batches.

	Abundance [%]					
Isotope	Natural Se	Initial ^{82}Se	Zn^{82}Se	Primary	Secondary	Tertiary
^{74}Se	0.87	< 0.01	0.01(1)	0.01(1)	0.11(1)	0.01(1)
^{76}Se	9.36	< 0.01	0.09(1)	0.11(1)	1.19(6)	0.08(1)
^{77}Se	7.63	< 0.01	0.07(1)	0.09(1)	1.00(5)	0.07(1)
^{78}Se	23.8	< 0.01	0.25(1)	0.29(1)	3.19(16)	0.21(1)
^{80}Se	49.6	3.67(14)	4.47(22)	4.18(21)	10.1(5)	4.52(23)
^{82}Se	8.73	96.3(3)	95.1(5)	95.3(3)	84.4(4)	95.6(3)

in this facility. Therefore there was no possibility to disrupt an initial level of the ^{82}Se isotope enrichment. The change in the isotopic composition of selenium at the stage of Zn^{82}Se crystals with respect to the initial highly enriched ^{82}Se with no admixture of light selenium isotopes can be explained as follows. To enhance the scintillating light yield of ZnSe crystals, Al is typically added as a dopant at the level of hundreds of ppm. To prepare the dopant mixture that would be uniformly distributed along the crystal ingots, a dedicated ZnSe crystal highly doped with Al, but produced from selenium with natural isotopic abundance, was grown. Then, this ZnSe:Al crystal was smashed to a fine powder form and added in a fixed amount to each Zn^{82}Se charge load. Hence, one could see the presence of selenium light isotopes in Zn^{82}Se crystals and recovered from the primary batch selenium and tertiary batch from processed water.

The largest deviation from the initial level of the ^{82}Se isotope enrichment is observed for the secondary batch, which is recovered from residuals collected from the inner volume of several furnaces used for Zn^{82}Se crystals growth, and from other material supposed to contain enriched Se collected from the growth site. However, since the Zn^{82}Se crystals were grown in furnaces which are routinely and actively used for production of ZnSe crystals from natural selenium, the collected residuals were containing selenium of natural isotopic composition in high amount. This leads to substantial reduction of the ^{82}Se enrichment level.

4.3 Radiopurity

The internal radioactive contamination of the extracted and purified ^{82}Se is compared to initial materials (Zn and ^{82}Se) and to the Zn^{82}Se crystals operated as scintillating bolometers.

The initial materials (Zn and ^{82}Se) along with the extracted ^{82}Se after recovery and purification were measured with the same ultra-low-background high-purity germanium detector (ULB-HPGe). These measurements were done in the STELLA (SubTerranean Low-Level Assay) facility at LNGS, providing an average shielding of 3600 m water equivalent against cosmic muons [31]. The ULB-HPGe detector was a coaxial p-type germanium detector with an active volume of approximately 400 cm^3 optimized for a high counting efficiency over a wide energy range. The energy resolution was 2.0 keV at the 1332 keV line of ^{60}Co. To minimize the contribution of an external gamma background to the studied sample counting rate, the ULB-HPGe detector is shielded with a 20-cm-thick layer of

2023 JINST 18 P04035

low-radioactivity lead and a 5 cm of OFHC (Oxygen Free High Conductivity) copper. The whole setup is continuously flushed with high-purity boil-off nitrogen to reduce the contribution of the environmental radon to the detector counting rate. Further details on the experimental setup and detector performance can be found in [31]. The initial Zn metal (10.08 kg) and ^{82}Se (2.50 kg) in the shape of few-mm-diameter granules were placed in a polypropylene Marinelli type [32] containers (GA-MA Associates, type 441G and 141G, respectively) above the end-cap of the ULB-HPGe detector. Spectra of internal radioactive contamination were acquired for 827.7 h and 1798.2 h, respectively. The extracted ^{82}Se ingots (6.51 kg) from the recovery process described above were fractured into approximately 5-mm-diameter pieces in a glovebox under inert atmosphere of high purity nitrogen and placed in a custom Marinelli container for the measurement over 1488.5 h. All measured results on radiopurity of the initial Zn, ^{82}Se and recovered ^{82}Se, along with the radiopurity of the Zn^{82}Se crystals retrieved from long-term measurements performed in the framework of the CUPID-0 experiment [33] are given in table 3.

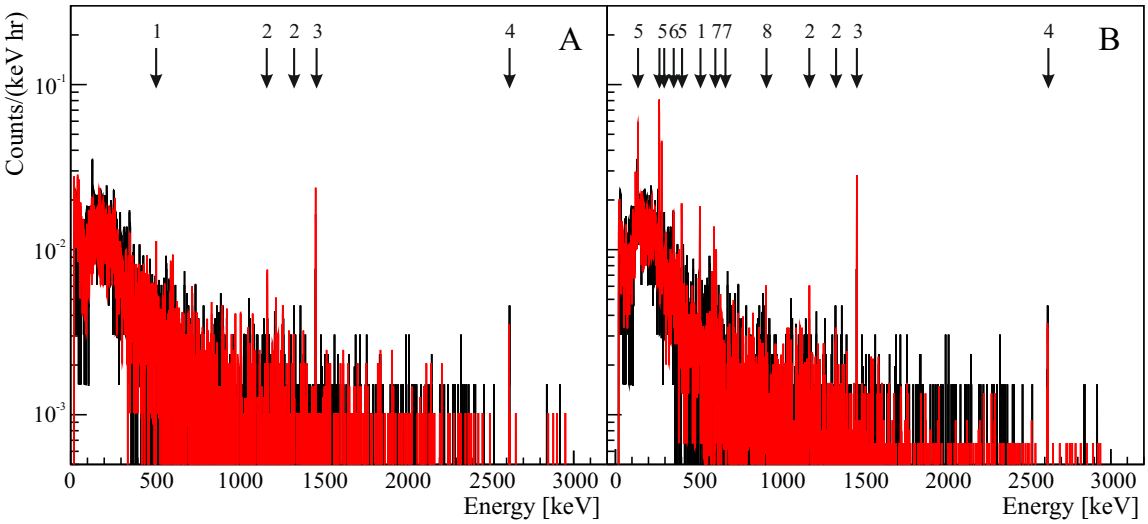

Figure 2. Gamma spectra of the measured Se samples (red) and background (black) for the initial ^{82}Se beads (A) and recovered ^{82}Se of (primary + secondary) batches (B) normalized to hour of background run time. The most prominent gamma lines in spectra are labeled as follows: 1) 511 keV annihilation peak; 2) 1173 and 1332 keV lines of ^{60}Co from the detector background; 3) 1461 keV line of ^{40}K; 4) 2615 keV line of ^{208}Tl from ^{232}Th decay chain; 5) 121, 136, 265, 280 and 401 keV lines of ^{75}Se; 6) 352 keV line of ^{214}Pb from ^{238}U chain; 7) 596 and 635 keV lines of ^{74}As; 8) 911 keV line of ^{228}Ac from ^{232}Th chain.

No evidence of activities of daughter nuclides from the natural decay chains of ^{232}Th, ^{235}U, and ^{238}U was observed in samples of the initial Zn and ^{82}Se, resulting in the placement of upper limits (90% confidence level (C.L.)) at the level of less than few mBq/kg. Moreover, only limits on the activity of other commonly observed nuclides, in particular for ^{40}K from natural radioactivity, ^{60}Co produced by cosmogenic activation, and anthropogenic ^{137}Cs, are reported. A significant activity of some specific isotopes such as ^{54}Mn, ^{57}Co, ^{57}Co, ^{58}Co, ^{65}Zn (in the Zn sample), and ^{75}Se (in the initial ^{82}Se sample) are at the mBq/kg level. These isotopes are produced by cosmogenic activation via neutron spallation on naturally occurring zinc and selenium isotopes. Spectra measured from the ULB-HPGe detectors normalized per keV per hour of equivalent of background acquiring time

2023 JINST 18 P04035

Table 3. Radiopurity of the initial Zn [34], the initial enriched ^{82}Se [30], Zn^{82}Se crystals [33], and the recovered ^{82}Se from the primary and secondary batches measured together. For Zn^{82}Se the activity of ^{234}Th from the ^{238}U chain is not directly presented in [33].

	Activity [mBq/kg]			
Radionuclide (Chain)	Initial Zn	Initial ^{82}Se	Zn^{82}Se crystals	Recovered ^{82}Se
^{40}K	< 0.38	< 0.99	0.085(4)	1.3(3)
^{54}Mn	0.11(2)			
^{56}Co	0.08(2)			
^{57}Co	0.20(9)			
^{58}Co	0.22(4)			
^{60}Co	< 0.036	< 0.065	0.014(3)	< 0.031
^{65}Zn	5.2(6)		0.352(6)	
^{74}As				0.30(2)
^{75}Se		0.11(4)		0.70(8)
^{137}Cs	< 0.033			< 0.022
^{228}Ra (^{232}Th)	< 0.095	< 0.061	0.00274(10)	< 0.10
^{228}Th (^{232}Th)	< 0.036	< 0.11	0.0120(3)	0.06(2)
^{235}U (^{235}U)	< 0.091	< 0.074	0.00053(7)	< 0.0072
^{234}Th (^{238}U)	< 6.2	< 6.2		< 7.4
^{234m}Pa (^{238}U)	< 4.7	< 3.4	0.00551(10)	2(1)
^{226}Ra (^{238}U)	< 0.066	< 0.11	0.0154(2)	0.07(2)
^{210}Pb (^{238}U)			0.00705(16)	

is shown in figure 2 for the initial ^{82}Se beads (left, A) and recovered ^{82}Se of primary+secondary batches (right, B).

The CUPID-0 background model, established and studied in detail in [33], indicates that the internal contamination of Zn^{82}Se crystals is much lower than the activity limits reported from the initial Zn and ^{82}Se assays. This enhancement of Zn^{82}Se radiopurity provides strong evidence of the segregation of impurities occurring during the crystal growth process. This effect was also observed earlier, see for instance [35]. In addition to a very low radioactive contamination, the secular equilibrium in ^{232}Th and ^{238}U decay chains is observed to be broken, which is already reported for many low-background crystals [36, 37].

In the recovered ^{82}Se sample some activity of ^{40}K and daughter nuclides of natural ^{232}Th and ^{238}U decay chains were detected at the level of few mBq/kg. Secular equilibrium is also broken in this ^{82}Se sample suggesting different dynamics of various elements during purification due to their different chemical properties. Apart from the natural radioactive nuclides, in the extracted selenium the cosmogenically-activated isotopes ^{74}As and ^{75}Se were observed.

To determine the possible origin of these two cosmogenically-activated nuclei, we have considered two time periods in which a high neutron or cosmic muon fluxes could occur that might

2023 JINST 18 P04035

cause the material activation. They are: 1) transportation of the selenium-containing waste by plane to the recovery site; 2) above-ground long-term storage at LNGS of the recovered ^{82}Se ingots in sealed quartz ampules, followed by the sample preparation in the above-ground chemistry lab for a radiopurity assay.

The selenium-containing waste were delivered by plane to the recovery site in March, 2017. The recovery process was performed through the summer and autumn 2017. Selenium was stored above-ground prior to and during the recovery process. The extracted and purified selenium was then shipped to LNGS by land transportation in November 2017, and from that time was stored in the underground site providing shielding against the cosmic muon flux up to a factor of 10^6. Thus, the most intense production of cosmogenically-activated isotopes ^{74}As and ^{75}Se may occur during the delivery of the selenium-containing waste by plane to the recovery site.

We have evaluated the possible cosmogenic activation of selenium with two different isotopic compositions (84% and 95%) using the ACTIVIA code [38]. We exploit the Gordon parametrization of the cosmic ray spectrum [39], and assume a 10 hours flight at 10000 m altitude. The results are reported in table 4, where the calculated activities are presented in terms of mBq/kg at the start of the selenium sample cooling-down (after the flight in March 2017). It should also be noted, that listed values of cosmogenic activation are expected to be correct at the order-of-magnitude level given typical uncertainty budgets in such calculations [40]. The cosmogenic activation is negligible for Mn, Co, and Zn isotopes. At the same time, activities of ^{73}As, ^{74}As, and ^{75}Se isotopes were estimated at the mBq/kg level. Taking into account half-lives of these isotopes (80.3 d, 17.8 d, and 118.5 d, respectively), their activities should be highly suppressed by the time of ULB-HPGe screening of the extracted selenium sample in March 2021, since a period of more than ten half-lives passed even for the long-lived ^{75}Se. Therefore, the material activation caused by air transportation cannot explain the observed activities of ^{74}As and ^{75}Se isotopes.

As mentioned, the recovered and purified ^{82}Se was shipped to LNGS by land transportation in November 2017, and from then stored in the underground site. First radioassay of this enriched material was planned for early 2020, and the material was brought to above-ground laboratory in February 2020. However, due to COVID-19 restrictions and limited access to surface and underground laboratories at LNGS, the ^{82}Se ingots were stored for approximately 9 months at the above-ground lab. Only after that period the sample preparation for low-background measurements was restarted. To estimate the effect of the above-ground storage at LNGS altitude on the material activation, a set of calculations using the ACTIVIA code were performed focusing on the induced activities of ^{73}As, ^{74}As, and ^{75}Se isotopes. The results are reported in table 5, where the calculated activity is presented in terms of mBq/kg after 270 days of exposure to cosmic rays at LNGS altitude followed by a 180 day cool-down period at the underground site prior ULB-HPGe measurements. The activity of the ^{75}Se isotope, evaluated taking into account a long-term above-ground exposure, reconstructs well the experimentally-observed value (0.7 mBq/kg) within a factor 2, while the estimated activities of ^{73}As and ^{74}As nuclei are many orders of magnitude below of the experimentally-observed values.

Moreover, to exclude the possibility that chemical impurities of As, Te, and Ba present at the $O(1 - 100)$ ppm in the recovered selenium (see table 1) could result in an additional counting rate of ^{73}As and ^{74}As isotopes, a complimentary calculation with the ACTIVIA code was performed. It was found that the induced cosmogenic activation of ^{73}As and ^{74}As in these impurity elements occur at the order of 10^{-7} mBq/kg or well below. Thus, the presence of As, Te, and Ba chemical impurities

2023 JINST 18 P04035

cannot explain the extra counting rate of these two cosmogenic isotopes. This contradiction between the experimentally observed and calculated activities of ^{73}As and ^{74}As suggests the existence of an alternative reaction for the production of these isotopes that is likely not included in the ACTIVIA code and should be further studied in detail. It can additionally be noted that these cosmogenic isotopes were not observed in the CUPID-0 experiment [41], so it is likely that they originate from the secondary batch of the recovered ^{82}Se.

Table 4. Cosmogenic activation of the selenium samples at 84% and 95% isotopic enrichment of ^{82}Se directly after transportation by plane, calculated using the ACTIVIA code [38]. No cool-down period is considered in these calculations. Activities are expressed in mBq/kg, while half-lives in days.

		Activity [mBq/kg]	
Isotope	$T_{1/2}$ [days]	84% of ^{82}Se	95% of ^{82}Se
^{54}Mn	312	1.4×10^{-3}	1.3×10^{-3}
^{56}Co	78.8	5.3×10^{-4}	2.7×10^{-4}
^{57}Co	271	8.3×10^{-4}	5.5×10^{-4}
^{58}Co	70.8	7.3×10^{-3}	5.8×10^{-3}
^{60}Co	1925.2	3.8×10^{-4}	4.0×10^{-4}
^{65}Zn	244.1	8.4×10^{-3}	6.2×10^{-3}
^{73}As	80.3	0.3	0.2
^{74}As	17.8	1.2	0.8
^{75}Se	118.5	0.3	0.2

Table 5. Cosmogenic activation of the selenium samples at 84% and 95% isotopic enrichment of ^{82}Se after 270 days of exposure to cosmic rays at LNGS altitude and 180 days of cool-down period at the underground site prior starting the ULB-HPGe measurements, calculated using the ACTIVIA code [38]. Activities are expressed in mBq/kg, while half-lives in days.

		Activity [mBq/kg]	
Isotope	$T_{1/2}$ [days]	84% of ^{82}Se	95% of ^{82}Se
^{73}As	80.3	0.3	0.2
^{74}As	17.8	1.2×10^{-3}	8.0×10^{-4}
^{75}Se	118.5	0.5	0.5

5 Discussion and conclusions

A highly-effective method of enriched selenium extraction has been developed that works both for ZnSe crystals as well as for remnants occurring through the ZnSe crystal production chain and conditioning. This method is a combination of wet chemistry reactions followed by a multi-stage vacuum distillation. The big advantage of the wet chemistry stage is the possibility to work with a large mass of initial pieces of ZnSe crystals that significantly simplifies the preparation of Se-containing materials prior the extraction process; minimization of preparatory actions on materials

2023 JINST 18 P04035

containing any enriched isotope is preferable, since it reduces the possibility to introduce chemical and radio-contamination. Moreover, this technique allows the recovery of selenium from scraps and waste water collected during mechanical treatments of $Zn^{82}Se$ crystals (i.e. cutting, polishing, and re-polishing with a fine, radiopure 1.5-μm-grain size SiO_2 powder). The preparatory actions in our case require only a separation of the entire remnant mass on suitable portions of material with a weight of approximately 300 g. Further improvements beyond the steps performed in this study, particularly on the wet chemistry reactions stage, could be achieved through: a) performing all chemical reactions in a clean room environment with air-quality control leading to a reduction of the radon concentration in the air; b) utilizing only quartz and Teflon lab-ware; c) utilizing ultra-pure water, along with ultra-pure re-distilled nitric and hydrochloric acids.

It is demonstrated that the selenium recovery technique developed here is preserving the level of isotopic enrichment of the initial ^{82}Se when comparing with the primary and tertiary batches. It could therefore be used in future campaigns for ^{82}Se isotope recovery and recycling.

The chemical purity of the primary batch is comparable to the initial ^{82}Se isotope used for the $Zn^{82}Se$ crystal growth. The recovery efficiency is estimated to be no less than 86.4% (and potentially can be higher than 94.7%) for enriched selenium from the primary processing with a high chemical purity (more than 99.999%). After the multi-stage vacuum distillation, the selenium ingots were condensed in sealed quartz ampules, proving to be an ideal way to store the recovered enriched material safely to prevent any possible chemical contamination and reaction with environmental humidity or air. The chemical purity of the secondary batch (more than 99.99%) is only slightly lower than the purity level achieved for the primary batch, showing only a relatively high contamination by Te and Si at the level of 57 and 33 ppm, respectively. This can be explained as the secondary batch mostly contains materials collected in the inner volume of furnaces that are actively used for a commercial ZnSe crystal production (commercial ZnSe is typically activated with tellurium to enhance its light yield). Additionally, the similarity in chemical properties of Te to Se leads to higher chemical involvement of Te in the wet chemistry stage rather than its separation. The tertiary batch has a chemical purity only at the level of 99.95%, caused by a more slow and complex reaction at the wet chemistry stage in the presence of a high concentration of a fine SiO_2 powder during initial selenium dissolution, as well as a different vacuum distillation process without gas treatment of the boiled selenium. Nevertheless, this batch could be used in some applications where a high level of ^{82}Se isotope enrichment would play more critical role than the ultimate level of its chemical purity.

The radiopurity of the extracted selenium for the primary and secondary batches together confirms the presence of ^{40}K and progeny of ^{232}Th and ^{238}U decay chains at the level of few mBq/kg. Unfortunately, separate measurements were not performed, although it is likely that this radioactive contamination is caused mostly by the secondary batch having a lower chemical purity and having been collected in the environment in touch with materials of low radiopurity (carbon felt, stainless steel, graphite, etc.). Moreover, a high concentration of Ca (7.0 ppm) and Ba (0.5 ppm) in the secondary batch suggests the likely presence of radium due to similarity in chemical properties and resulting in its observed activity. In order to be used in any low-background application this batch of the extracted selenium should be subjected to an additional, dedicated vacuum distillation.

The observed activities of cosmogenically-activated ^{75}Se at the level of 0.7 mBq/kg can be explained by neutron spallation on selenium nuclei, confirmed with good accuracy by ACTIVIA calculations. At the same time, activities of ^{73}As and ^{74}As cosmogenic isotopes, are still not

2023 JINST 18 P04035

fully understood. It is difficult to explain their activities in the selenium sample only by neutron spallation. We suggest that an alternative reaction or reactions from neutron spallation could lead to a continuous production rate of those isotopes even in a selenium sample being stored deep underground. Further studies of the radiopurity of the recovered enriched ^{82}Se isotope is ongoing within long-term low-background measurement with a ULB-HPGe spectrometer.

In conclusion, the highly effective extraction technique (with the yield no less than 86.4%, that potentially can be higher than 94.7%) presented here allows for the recovery of selenium of different levels of ^{82}Se enrichment (84% and 95.5%) and various chemical- and radio-purity levels. This recovered selenium could be used to produce more Zn^{82}Se scintillating crystals in case of an extension of the CUPID-0 research program or other low-background experiments (such as SELENA [42]) focused on studies of rare nuclear processes and seeking enriched selenium isotopes.

Acknowledgments

We appreciate the fruitful collaboration with URENCO Netherland B.V. and especially Dr. Peter Groen. We also appreciate helpful discussions and expert technical support on selenium purification from M. F. Churbanov, G. E. Snopatin, and M. V. Sukhanov. BB is supported by the Natural Sciences and Engineering Research Council of Canada (NSERC). SSN is supported by the Arthur B. McDonald Canadian Astroparticle Physics Research Institute.

References

[1] G.L. Fogli, E. Lisi, A. Marrone and A. Palazzo, *Global analysis of three-flavor neutrino masses and mixings*, *Prog. Part. Nucl. Phys.* **57** (2006) 742 [hep-ph/0506083].

[2] M.J. Dolinski, A.W.P. Poon and W. Rodejohann, *Neutrinoless double-beta decay: Status and prospects*, *Ann. Rev. Nucl. Part. Sci.* **69** (2019) 219 [arXiv:1902.04097].

[3] F.F. Deppisch, L. Graf, J. Harz and W.-C. Huang, *Neutrinoless double beta decay and the baryon asymmetry of the universe*, *Phys. Rev. D* **98** (2018) 055029 [arXiv:1711.10432].

[4] A. Giuliani et al., *Double beta decay APPEC committee report*, arXiv:1910.04688.

[5] KamLAND-Zen collaboration, *Search for Majorana neutrinos near the inverted mass hierarchy region with KamLAND-Zen*, *Phys. Rev. Lett.* **117** (2016) 082503 [*Addendum ibid.* **117** (2016) 109903] [arXiv:1605.02889].

[6] Theia collaboration, *THEIA: an advanced optical neutrino detector*, *Eur. Phys. J. C* **80** (2020) 416 [arXiv:1911.03501].

[7] EXO-200 collaboration, *Search for neutrinoless double-β decay with the complete EXO-200 dataset*, *Phys. Rev. Lett.* **123** (2019) 161802 [arXiv:1906.02723].

[8] NEXT collaboration, *Measurement of the ^{136}Xe two-neutrino double-β-decay half-life via direct background subtraction in NEXT*, *Phys. Rev. C* **105** (2022) 055501 [arXiv:2111.11091].

[9] PandaX-II collaboration, *Searching for neutrino-less double beta decay of ^{136}Xe with PandaX-II liquid xenon detector*, *Chin. Phys. C* **43** (2019) 113001 [arXiv:1906.11457].

[10] nEXO collaboration, *nEXO: neutrinoless double beta decay search beyond 10^{28} year half-life sensitivity*, *J. Phys. G* **49** (2022) 015104 [arXiv:2106.16243].

2023 JINST 18 P04035

[11] NEXT collaboration, *Sensitivity of a tonne-scale NEXT detector for neutrinoless double beta decay searches*, *JHEP* **2021** (2021) 164 [arXiv:2005.06467].

[12] M. Pierre, *Neutrinoless double beta decay search with XENON1T and XENONnT*, *Nuovo Cim. C* **45** (2022) 17.

[13] LEGEND collaboration, *The Large Enriched Germanium Experiment for Neutrinoless Double Beta Decay (LEGEND)*, *AIP Conf. Proc.* **1894** (2017) 020027 [arXiv:1709.01980].

[14] AMoRE collaboration, *Technical design report for the AMoRE* $0\nu\beta\beta$ *decay search experiment*, arXiv:1512.05957.

[15] C. Augier et al., *Final results on the* $0\nu\beta\beta$ *decay half-life limit of* ^{100}*Mo from the CUPID-Mo experiment*, *Eur. Phys. J. C* **82** (2022) 1033 [arXiv:2202.08716].

[16] CUPID collaboration, *Toward CUPID-1T*, arXiv:2203.08386.

[17] CUPID collaboration, *Final result on the neutrinoless double beta decay of* ^{82}*Se with CUPID-0*, *Phys. Rev. Lett.* **129** (2022) 111801 [arXiv:2206.05130].

[18] I. Dafinei et al., *Production of* ^{82}*Se enriched zinc selenide (ZnSe) crystals for the study of neutrinoless double beta decay*, *J. Cryst. Growth* **475** (2017) 158 [arXiv:1702.05877].

[19] S. Pirro and P. Mauskopf, *Advances in bolometer technology for fundamental physics*, *Ann. Rev. Nucl. Part. Sci.* **67** (2017) 161.

[20] D. Poda, *Scintillation in low-temperature particle detectors*, *Physics* **3** (2021) 473.

[21] E. A. Scott et al., *Phonon scattering effects from point and extended defects on thermal conductivity studied via ion irradiation of crystals with self-impurities*, *Phys. Rev. Mater.* **2** (2018) 095001.

[22] N.E. Booth, B. Cabrera and E. Fiorini, *Low-temperature particle detectors*, *Ann. Rev. Nucl. Part. Sci.* **46** (1996) 471.

[23] I. Dafinei et al., *Low Temperature Scintillation in ZnSe Crystals*, *IEEE Trans. Nucl. Sci.* **57** (2010) 1470.

[24] M. Manutchehr-Danai, *Bridgman-stockbarger technique*, in *Dictionary of gems and gemology*, Springer, Berlin **111** (2009).

[25] P. Rudolph, N. Schäfer and T. Fukuda, *Crystal growth of ZnSe from the melt*, *Mater. Sci. Eng. R: Rep.* **15** (1995) 85.

[26] J. Jannek and J. Meyer, *Eine neue bestimmung des atomgewichtes des selens*, *Zeitschrift für anorganische Chemie* **83** (1913) 51.

[27] O. Höunigschmid and W. Kapfenberger, *Revision des atomgewichtes des selens synthese des silberselenids*, *Zeitschrift für anorganische und allgemeine Chemie* **212** (1933) 198.

[28] V.S. Shiryaev et al., *Removal of barium impurities from selenium by vacuum distillation*, *Inorg. Mater.* **46** (2010) 314.

[29] Y.P. Kirillov et al., *Modeling of the evaporation of liquids and condensation of their vapor during distillation*, *Inorg. Mater.* **52** (2016) 1183.

[30] LUCIFER collaboration, *Double-beta decay investigation with highly pure enriched* ^{82}*Se for the LUCIFER experiment*, *Eur. Phys. J. C* **75** (2015) 591 [arXiv:1508.01709].

[31] M. Laubenstein, *Screening of materials with high purity germanium detectors at the Laboratori Nazionali del Gran Sasso*, *Int. J. Mod. Phys. A* **32** (2017) 1743002.

[32] R.F. Hill, G.J. Hine and L.D. Marinelli, *The quantitative determination of gamma radiation in biological research*, *Am. J. Roentgenol. Radium. Ther.* **63** (1950).

2023 JINST 18 P04035

[33] CUPID collaboration, *Background Model of the CUPID-0 Experiment*, *Eur. Phys. J. C* **79** (2019) 583 [arXiv:1904.10397].

[34] F. Bellini et al., *Search for double β-decay modes of ^{64}Zn using purified zinc*, *Eur. Phys. J. C* **81** (2021) 106 [arXiv:2012.05873].

[35] F.A. Danevich et al., *Effect of recrystallisation on the radioactive contamination of $CaWO_4$ crystal scintillators*, *Nucl. Instrum. Meth. A* **631** (2011) 44.

[36] F.A. Danevich and V.I. Tretyak, *Radioactive contamination of scintillators*, *Int. J. Mod. Phys. A* **33** (2018) 1843007 [arXiv:1804.00653].

[37] P. Belli et al., *Radioactive contamination of SrI_2(Eu) crystal scintillator*, *Nucl. Instrum. Meth. A* **670** (2012) 10 [arXiv:1111.5505].

[38] J.J. Back and Y.A. Ramachers, *ACTIVIA: Calculation of isotope production cross-sections and yields*, *Nucl. Instrum. Meth. A* **586** (2008) 286 [arXiv:0709.3472].

[39] M.S. Gordon et al., *Measurement of the flux and energy spectrum of cosmic-ray induced neutrons on the ground*, *IEEE Trans. Nucl. Sci.* **51** (2004) 3427.

[40] V.A. Kudryavtsev, *Cosmogenic activation: Recent results*, *AIP Conf. Proc.* **1921** (2018) 090004.

[41] O. Azzolini et al., *CUPID-0, challenges and achievements in the struggle of 0-background double-beta decay experiments*, *Nucl. Instrum. Meth. A* **936** (2019) 519.

[42] A.E. Chavarria et al., *Snowmass 2021 White Paper: The Selena Neutrino Experiment*, [arXiv:2203.08779].

2023 JINST 18 P04035